

Multiple-Threshold Estimators for Impulsive Noise Suppression in Multicarrier Communications

Nikola Rožić¹, Senior Member, IEEE, Paolo Banelli², Member, IEEE, Dinko Begušić, Senior Member, IEEE, and Joško Radić¹, Member, IEEE

Abstract—Multicarrier wireless communication systems, which usually operate over frequency-selective fading channels, are practically also impaired by environmental impulsive noise. In order to boost the signal-to-noise power ratio (SNR) at the receiver, this paper proposes and analyzes nonlinear estimators based on the multiple thresholding, with associated piecewise attenuation, or clipping, of the received signal amplitude. The proposed approach exploits a new heuristic criterion to set the thresholds. Although the obtained thresholds are slightly suboptimal in output SNR, the proposed approach has the nice and useful property to allow closed-form analytical derivations for both the threshold(s) and the associated attenuating/clipping parameters, when a Gaussian source is impaired by an impulsive noise. Such a quite general class of estimators, which could be applied also in other scenarios, is particularly attractive for orthogonal frequency division multiplexing communication systems in the presence of additive multicomponent impulsive noise. We are also letting to derive closed-form expressions for the output SNR in frequency-selective multipath fading channels. The SNR performance and the associated symbol error rate have been compared with those of more traditional blanking, clipping, and clipping-blanking processors. Specifically, analytical and simulation results, carried out for Class-A and symmetrical alpha-stable (S α S) impulsive noise, show that the proposed threshold-based suppressors are superior to the traditional ones. Furthermore, as the number of thresholds increases, the proposed estimators closely approach the performance of the optimal minimum mean square error Bayesian estimator. However, as it is shown, in practical conditions only few thresholds are necessary.

Index Terms—Impulsive noise suppression, Bayesian estimator, optimal thresholding, non-linear signal processing, fading channels, OFDM systems.

I. INTRODUCTION

THE performance of digital communication systems, employed in cellular, broadcasting, and wireless access networks, can be significantly degraded by adverse channel conditions and interferences, which characterize wireless

communications in urban environments. These interferences are typically modeled as non-Gaussian impulsive noises [1]–[3], such as the Middleton’s Class-A noise that, together with the associated suppression techniques, has been widely investigated in the past (see [4]–[8] and references therein). Although multicarrier modulations, currently employed in most of the wireless communication systems, are inherently more resistant to impulsive noise (ImpN) than single carrier modulations, the counteraction of the performance degradation caused by ImpN is still a challenging research area for communication engineers [9]–[11]. Actually, countermeasures for Class-A noises can be easily generalized to any scenario characterized by multi-component Gaussian mixture noises [7], [8], and consequently also to alpha-stable impulsive noises, which can be modeled as a Gaussian mixture as well [12]–[14]. Assuming a Gaussian source impaired by memoryless ImpN, optimum system performance in terms of mean-squared error (MSE) and signal-to-noise power ratio (SNR) can be achieved by applying a Bayesian signal estimator [15]. Specifically, the optimal Bayesian estimator (OBE) for real-valued Gaussian mixture noise has been proposed in [8], and successively extended to complex signals in [9]. Although the OBE guarantees optimal MSE and SNR for uncorrelated ImpN, in some cases its implementation in practical receivers may be cumbersome or not attractive. For instance, if ImpN suppression is performed before A/D conversion, an analogic solution may be too complex, while if impulse noise suppression is performed after A/D conversion, the computational complexity and the system latency may be relatively high, especially for simple low-cost devices [8], [15]. Consequently, less complex solutions are typically based on signal thresholding, associated with blanking (nulling) [6], [8], [10], [16], clipping [7], [8], [15], or their combinations [5], [7], [11], [17]. Recently, an MMSE estimator, constrained to a given quantization resolution of the noisy observations [15], has been proved to converge to the MMSE optimal solution, e.g., the OBE, which conversely uses an infinite resolution of the observation. Although all the mentioned techniques can be used in any system impaired by additive ImpN, their application to OFDM, or any other multicarrier wireless system, is more challenging when the system is also affected by frequency-selective fading channels, as we will clarify.

Thus, this paper focuses on OFDM signals which are employed in a wide class of multicarrier systems, including asymmetric digital subscriber lines (ADSL) [18], power-line communications (PLC) [19], 4G cellular systems

Manuscript received September 16, 2017; accepted December 28, 2017. Date of publication January 15, 2018; date of current version February 7, 2018. The associate editor coordinating the review of this manuscript and approving it for publication was Prof. Amir Asif. This work was supported by the University of Split, FESB project “Advanced Networking Technologies and Systems” 273 13-18. (Corresponding author: Nikola Rožić.)

N. Rožić, D. Begušić, and J. Radić are with the Department of Electronics and Computing, FESB, University of Split, Split 21000, Croatia (e-mail: rozic@fesb.hr; begusic@fesb.hr; radic@fesb.hr).

P. Banelli is with the Department of Engineering, University of Perugia, Perugia 06125, Italy (e-mail: paolo.banelli@unipg.it).

Color versions of one or more of the figures in this paper are available online at <http://ieeexplore.ieee.org>.

Digital Object Identifier 10.1109/TSP.2018.2793895

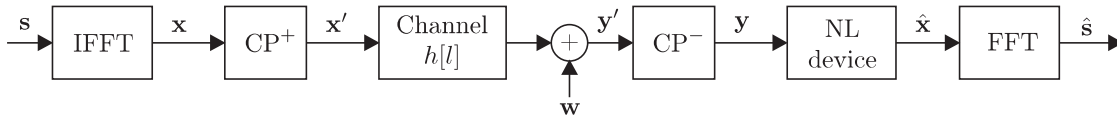


Fig. 1. Block scheme of system model.

(UMTS-LTE), broadcasting (DVB-T) [5], and wireless local area networks (WiFi) [20], [21], although similar conclusions and results can be easily extended to any multicarrier system.

As principal contribution, we propose a set of novel multiple thresholding-based devices for complex-valued signals, which can easily trade-off performance for complexity, by using a lower or higher number of thresholds. To our best knowledge the only result reported in the literature related to multiple thresholding is [15]. Other papers, including one of the most recent [17], typically only focus on blanking, clipping, or a mix of two estimators. Specifically, we propose and analyze the performance of piece-wise attenuators and piece-wise clippers, that we name multiple threshold Bayesian attenuating suppressor (BAS) and multiple threshold Bayesian clipping suppressor (BCS), respectively. We will show that these suppressors have the nice property to approximate the optimal MSE (and SNR) performance of the OBE, as the number of thresholds increases. This is partially in the spirit of [15], where however i) the thresholds have been not optimized according to the noise statistics (they were chosen either equi-spaced on the input dynamics, or by a Lloyd-Max quantization), ii) the associated output values can be only constant (i.e., clipped) within consecutive thresholds, iii) MSE and SNR closed-form results have been derived for signal and noise characterized by different *pdfs* with respect to those considered herein.

Conversely, a further contribution of this manuscript is the introduction of a novel and effective criterion to select the thresholds when the Gaussian OFDM signal is impaired by an ImpN modeled by a K-component Gaussian mixture model (K-GMM). In this case, the new criterion turns out to be not only performance-wise effective, but it also leads to closed-form analytical expression for the dependence of the thresholds (and the associated optimal attenuating/clipping values) on the system parameters (i.e., noise power, signal power, channel fading, etc.). This is a great advantage with respect to other MSE- or SNR-optimal thresholding methods, which actually require either numerical integration [6], [7] or iterative solution of fixed-point equations [8], [9]. This benefit is particularly useful in wireless communication systems that, in order to maximize the performance, should frequently adapt their thresholds and attenuating/clipping values to the evolution of frequency-selective fading channels [9].

Finally, the proposed framework lets also to derive closed-form analytical expressions for the output SNR of the proposed set of suppressors in the presence of any K-GMM ImpN. Simulation results corroborate the theoretical findings for the proposed BAS and BCS, whose performance in OFDM systems are compared with the OBE [9], as well as with some of the most popular suboptimal methods, including blanking and clipping-blanking

[6], [7], both in the presence of Class-A and S α S impulsive noises.

The rest of the paper is organized as follows: Section II briefly summarizes the system model and the impulsive noise K-GMM model. Section III resumes the optimal genie-aided estimator as well as the OBE, while Section IV describes the proposed threshold-based methods for signal detection interfered by impulsive noise. Section V derives analytical closed-form expressions for the output SNR, both for the optimal and the multiple thresholding estimators. Section VI and Section VII derive closed-form expressions for the proposed thresholds heuristics and the associated optimal attenuating/clipping values, respectively. Numerical and simulation results and system performance for OFDM system are presented in Section VIII together with comparison to existing ImpN suppressing methods. Finally, Section IX provides some concluding remarks.

II. SYSTEM AND NOISE MODELS

This section summarizes the communication and the ImpN models under investigation. Specifically, we focus on OFDM communications over frequency-selective multipath fading channels, while the ImpN model includes both the well known Middleton Class-A, and the bit less investigated α -stable model.

A. System Model

Let $\mathbf{s}_q = [s_q[0], s_q[1], \dots, s_q[N-1]]^T$ represent the q th frequency-domain symbol transmitted by an OFDM system with N orthogonal carriers, where the data $\{s_q[m]\}_{m=0, \dots, N-1}$ on different carriers are independent and, without restriction of generality, with zero mean and the same variance $\sigma_s^2 = E\{|s_q[m]|^2\}$. As well known, the OFDM symbol $\mathbf{x}_q = [x_q[0], x_q[1], \dots, x_q[N-1]]^T$ is generated in the time-domain by computing the inverse discrete Fourier transform (IDFT) of the data \mathbf{s}_q , as expressed by $\mathbf{x}_q = \mathbf{F}_N^H \mathbf{s}_q$, where \mathbf{F}_N is the N -point unitary DFT matrix [22], [23] and H is the Hermitian operator. Furthermore, to avoid inter-block interference and simplify channel equalization, a cyclic prefix (CP) is added to the OFDM block, generating $\mathbf{x}_q^{\text{cp}} = [x_q[N-L], \dots, x_q[N-1], x_q[0], x_q[1], \dots, x_q[N-1]]^T$ that, after D/A conversion and RF modulation, is transmitted through the channel.

Fig. 1 shows the discrete-time equivalent of the overall transmitter-receiver chain, which is affected by the N -length channel impulse response vector $\mathbf{h}_q = [h_q[0], h_q[1], \dots, h_q[L-1], 0, \dots, 0]^T$, where $h_q[l]$ is the l th discrete-time path of the channel during the q th OFDM block, and only the first L paths are actually different from zero. We assume a block-fading model for the channel, e.g., all the L active paths are modeled as time-invariant during the transmission of each OFDM block. We also assume that each path experiences a Rayleigh fading,

e.g., the challenging situation without any line-of-sight between transmitter and receiver, and that each channel path $\{h_q[l]\}$ is modelled as a complex, independent, zero-mean Gaussian random variable with stationary variance $\sigma_l^2 = E\{|h_q[l]|^2\}$. Anyway, extension of the proposed analysis to other fading scenarios is quite straightforward.

After CP removal, the OFDM received symbol $\mathbf{y}_q = [y_q[0], y_q[1], \dots, y_q[N-1]]^T$ is obtained by cyclic convolution with the channel, as expressed by

$$y_q[n] = \sum_{l=0}^{L-1} h_q[l] x_q[(n-l)_N] + w_q[n]. \quad (1)$$

In the frequency domain this corresponds to carrier by-carrier multiplication of the channel transfer function with the transmitted data, as expressed by

$$\mathbf{y}_q^{(f)} = \mathbf{F}_N \mathbf{y}_q = \text{diag}(\mathbf{h}_q^{(f)}) \mathbf{s}_q + \mathbf{w}_q^{(f)}, \quad (2)$$

where $\mathbf{h}_q^{(f)} = \sqrt{N} \mathbf{F}_N \mathbf{h}_q$ and $\mathbf{w}_q^{(f)} = \mathbf{F}_N \mathbf{w}_q$ are the frequency-domain channel response and noise, respectively, during the q th OFDM block.

As shown in Fig. 1, we envision that the ImpN suppression is performed in the time-domain, producing an estimated vector $\hat{\mathbf{x}}_q = g(\mathbf{y}_q; \boldsymbol{\pi}_q)$, where $g(\cdot)$ is the non-linear estimator to design and analyze, and $\boldsymbol{\pi}_q$ is a vector containing the value of a set of parameters during the q th OFDM block, such as the signal power $\sigma_{x_q}^2$, the noise power $\sigma_{w_q}^2$, etc., which inevitably should influence the behavior of the estimator. The idea is to counteract the noise impulses before DFT processing, which conversely by (2) would disperse the quite sparse time-domain impulses $w_q[n]$ over all the OFDM carriers in the frequency-domain, potentially impairing the demodulation of each transmitted symbol $\{s_q[m]\}_{m=0, \dots, N-1}$. Furthermore, motivated by low complexity requirements, we ignore any possible correlation between different time-domain impulses, thus focusing on instantaneous devices, as expressed by

$$\hat{x}_q[n] = g(y_q[n]; \boldsymbol{\pi}_q). \quad (3)$$

Further note that, due to their instantaneous nature these estimators cannot counteract the distortions induced by convolution (1) with the channel impulse response \mathbf{h}_q , which are by definition memory based. Consequently, as shown in Fig. 1, channel compensation is split from noise removal and performed in the frequency domain after DFT processing, by the classical per-subcarrier single-tap equalization that inspires the OFDM design [22], [23]. Anyhow, the knowledge of the channel impulse response \mathbf{h}_q , which should inform any channel equalizer, can be exploited also by the nonlinear impulse suppressor (NIS). Indeed, the power of the zero-mean received signal $y_q[n]$ is expressed by $\sigma_{y_q}^2 = \sum_{l=0}^{L-1} |h_q[l]|^2 \sigma_x^2 + \sigma_w^2$ where $\sigma_x^2 = E\{|x_q[n]|^2\}$ and $\sigma_w^2 = E\{|w_q[n]|^2\}$ are the transmitted OFDM signal and receiver noise powers, respectively. Thus, as further explained and motivated in the next sections, in the presence of a fading channel $\{h_q[l]\}_{l=0, \dots, L-1}$, any statistically designed NIS should adapt its response $g(y_q[n]; \boldsymbol{\pi}_q)$, from an OFDM block to another, to follow the channel fluctuations.

B. Impulsive Noise Models

A simple and widely used ImpN model [2], [7], [24], [25], assumes the presence, or absence, of a strong impulsive noise as the realization of two mutually exclusive events, with probability p_I and $1 - p_I$, respectively. Specifically, according to a Bernoulli-Gaussian (BG) distribution [24], this is a 2-GMM consisting of a thermal noise component $w_0 \sim G(w_0, \sigma_0^2)$ and an ImpN component $w_i \sim G(w_i, \sigma_I^2)$, with $\sigma_I \gg \sigma_0$, where $G(x, \sigma_x^2)$ is a zero-mean Gaussian probability density function (pdf) with variance σ_x^2 .

More generally, we can resort to a K-GMM [26], with pdf

$$f_W(w) = \sum_{k=0}^{K-1} p_k G(w, \sigma_k^2), \quad (4)$$

where $\{p_k\}_{k=0,1, \dots, K-1}$, with $\sum_{k=0}^{K-1} p_k = 1$, are the probabilities that an impulsive event is generated according to the k th Gaussian distribution. Thus, the component with $k=0$ represents the "only-thermal" noise event, which shows up with probability p_0 and average power σ_0^2 , while the statistical combination of the other events models the ImpN, which is manifest with probability $p_I = 1 - p_0$.

This paper focuses on two specific ImpN categories representable by (4), namely the Middleton's Class-A model [2], and the symmetric alpha-stable (S α S) model [27] that, under certain conditions, boils down to the Middleton's Class-B model [2]. However, it is important to note that the methods presented in this work are not restricted in any way to only Class-A and S α S models. The K-GMM model can be successfully applied to any ImpN distribution either estimated [3], [20], [28] and approximated by a K-GMM [29], or modeled with (4) [30], [31]. Thus, K-GMM impulsive noise is not assumed in order to restrict the analysis to solvable problems. Right the opposite, it is selected because K-GMM de-composes any random variable to a set of K mutually exclusive Gaussian variables [26] and, with enough high K , K-GMM can approximate any realistic distribution as close as required, while keeping the elegance of mathematical manipulation with Gaussian random variables. Generally, ML estimation of K-GMM parameters [29] also includes ML estimation of the number of mixture components K .

1) *Class A Impulsive Noise*: The Class-A model assumes $K = \infty$ in (4) and a relationship between the mixture variances σ_k^2 and the weighting coefficients p_k [32]. In short, this model is fully defined by a triplet of canonical parameters (σ_W^2, Γ, A) [33], where the variances of each component

$$\sigma_k^2 = \frac{k/A + \Gamma}{1 + \Gamma} \sigma_W^2 = \frac{k}{A} \sigma_I^2 + \sigma_0^2 = \left(1 + \frac{k}{A\Gamma}\right) \sigma_0^2 \quad (5)$$

and the associated Poisson distributed probabilities

$$p_k = e^{-A} A^k / k!, \quad (6)$$

are linked by the canonical parameter A . Actually the parameter A , which is known as the impulsiveness index, turns out to be the average number of mixture components, e.g., noise sources, that are simultaneously active at each time epoch, as easily verified by $A = E\{k\} = \sum_{k=0}^{\infty} k p_k$. This way, the total noise power $\sigma_W^2 = \sum_{k=0}^{\infty} p_k \sigma_k^2$, is split between the thermal noise power

$\sigma_0^2 = \Gamma\sigma_W^2/(1 + \Gamma)$ and the ImpN power $\sigma_I^2 = \sigma_0^2/\Gamma$, where clearly the canonical parameter Γ represents the power ratio among the two components. The total power σ_I^2 of the impulsive noise can be rather high, with Γ that in many realistic systems is in the range from 10^{-6} to 1, while A is typically in the range from 10^{-4} to 1 [34]. As shown in Sect. VIII, the sparsity of the noise impulses directly influences the performance of the estimator, which is generally characterized by an higher output SNR for decreasing values of the parameter A in (6).

Actually, for realistic systems, the K-GMM in (4) with $K \geq 10$, is a very good approximation of the Class-A model with $K = \infty$, if the truncated Poisson distribution \tilde{p}_k is properly re-normalized, e.g., $\tilde{p}_k = p_k / \sum_{k=0}^{K-1} p_k$ [16], [19]. Conversely, a 2-GMM is a good approximation of the Class-A model only when A and Γ are rather low.

2) *Alpha Stable Impulsive Noise*: the α -stable random variable (RV) has found wide interest in statistics and communications [27], [35], [36] due to its generality and ability to represent heavy-tailed (algebraic) distributions and impulsive noises. The *pdf* of the standard ($\gamma = 1, \mu = 0$) α -stable RV can be indirectly defined as the inverse Fourier transform of its characteristic function, as expressed by

$$f_W(w) = \frac{1}{2\pi} \int_{-\infty}^{\infty} e^{-t\alpha} \cos[wt + \beta t^\alpha \psi(t)] dt, \quad (7)$$

where

$$\psi(t) = \begin{cases} \tan \frac{\alpha\pi}{2} & \text{for } \alpha \neq 1 \\ \frac{2}{\pi} \log |t| & \text{for } \alpha = 1 \end{cases}.$$

However, an explicit analytical expression for its *pdf* does not exist, except for some specific values of α . The characteristic exponent $\alpha \in [0, 2]$ measures the tail thickness of $f_W(w)$, which is heavier for smaller values of α , and vice versa. The *pdf* with a minimal thickness ($\alpha = 2$) corresponds to the Gaussian *pdf*. For the skewness parameter $\beta = 0$, the distribution is symmetric about the center μ and it is called the *symmetric* α -stable (S α S) distribution. Due to a lack of an appropriate analytical expression for its *pdf*, the α -stable distribution can be analytically defined by an infinite mixture of Gaussians [13], [37], which in practice is useful to approximate by a finite scaled Gaussian mixture [12], [21].

This paper uses an efficient method [14] that exploits a number $K \in [3, 20]$ of components, which is based on the computations of the variances and the weighting factors that minimize the relative entropy between the K-GMM *pdf* and the S α S *pdf* over the support range $\pm A_N$.

It is interesting to note that when a symmetric α -stable signal is observed in the presence of an independent zero-mean Gaussian noise or vice versa, the resulting noise, which is typically named as S α S+G process [35], has a *pdf* that is conform to the Middleton Class B model [2].

III. OPTIMAL NON-LINEAR ESTIMATORS

According to the paradigm summarized in (3), our aim is to design simple, albeit effective, non linear estimators $g(\cdot)$ that work instantaneously on the received sample $y_q[n]$, by

exploiting statistical information on the useful components $\{x_q[\langle n - l \rangle_N]\}_{l=0, \dots, L-1}$ and the noise component $w_q[n]$. By Central Limit Theorem arguments, it is well known that the time-domain OFDM signal $x_q[n]$ is well modelled by a Gaussian *pdf* when the number of subcarriers N is sufficiently high [6]. Due to the fact that any OFDM receiver should be informed about the channel coefficients $\{h_q[l]\}_{l=0, \dots, L-1}$ in order to perform channel equalization, this channel knowledge can be exploited also at the NIS for effective impulse noise removal. Whichever is the known channel during the q th OFDM block, the useful component $r_q[n] = \sum_{l=0}^{L-1} h_q[l]x_q[\langle n - l \rangle_N]$ in (1) is still Gaussian distributed, as in the classical AWGN case, where $r_q[n] = h_0x_q[n]$. In the case of the frequency selective fading channels, the only difference is that the useful signal power $\sigma_{r_q}^2$ fluctuates from an OFDM block to another, according to the q th realization $\{h_q[l]\}_{l=0, \dots, L-1}$ of the channel. Thus, if all the N subcarriers transmit independent data¹ $s_q[n]$ [38], the time-domain signal power $\sigma_x^2 = E\{|x_q[n]|^2\}$ is stationary (after CP removal) and the conditional *pdf* of the useful component $r_q[n]$ at the NIS input, for a given channel, is expressed by

$$f_{r_q|h_q}(r, \mathbf{h}_q) = G(r, \sigma_{r_q}^2), \quad (8)$$

where $\sigma_{r_q}^2 = E\{|r_q[n]|^2\} = G_q\sigma_x^2$, and $G_q = \sum_{l=0}^{L-1} |h_q[l]|^2$ is the channel power attenuation for the q th OFDM block. In the following sections, due to the fact that statistical formulation (and solution) of the estimation problem is formally equivalent in the two cases, for notation simplicity we will denote by x and by w the two random variables that at each time epoch represent, respectively, the useful signal and the interfering impulsive noise, where $x = k_0x[n]$ in flat AWGN channels and $x = r_q[n]$ in frequency selective channels.

A. Genie-Aided Estimator (GAE)

Assuming that the impulsive noise is distributed according to the K-GMM *pdf* in (4), we consider genie-aided estimator (GAE) the Bayesian MMSE estimator that assumes also knowledge of the state of the underlying noise generation process. This means that, having modeled the impulsive noise as the evidence of properly weighted, mutually exclusive, Gaussian events, the GAE assumes to know which is the k th Gaussian component of the (*pdf*) mixture that is active at each time epoch, and produced the actual noise. Thus, conditionally on this knowledge, the received signal $y = x + w|_k$ is the sum of two zero-mean independent Gaussian RVs with variances σ_x^2 and σ_k^2 , respectively. In this case, the MMSE estimator is well known to be linear in the observation y , and simply expressed by

$$\hat{x}|_k(y) = g_{\text{GAE}}(y) = \frac{\sigma_x^2}{\sigma_x^2 + \sigma_k^2} y = \rho_k y. \quad (9)$$

Thus, the linear GAE simply changes its slope at every time-epoch according to its assumed perfect (and not realistic) knowledge of the present noise state, e.g., σ_k^2 . Note that (9) holds true also for the real and imaginary parts of the complex-valued

¹digital systems regularly use scrambling before modulation.

signals we are dealing with in wireless OFDM. Actually, it is straightforward to generalize the GAE in (9) to complex-valued RVs and a K -component complex Gaussian noise mixture, as expressed by

$$g_{\text{GAE}^*}(y) = \rho_k |y| e^{j \arg(y)}, \quad (10)$$

where $\rho_k = \frac{1}{1+\gamma_k}$, and $\gamma_k = \sigma_k^2 / \sigma_x^2$ is the power ratio among the noise and the useful signal. Basically, the conditionally linear estimator is applied to the signal envelope $|y|$. The use of the GAE in practical systems is not feasible due to the fact that the receiver does not know the power ratio γ_k at every time epoch, i.e., the receiver ignores which is the actual noise component k that affects the received signal y . Thus, the MSE performance of the GAE, which assumes perfect noise state information (NSI), represents a lower-bound for any other estimator, which can approach the GAE performance as long as it is able to reliably estimate γ_k at each time epoch. This could be done for instance by exploiting other side information, such as the correlation of the impulsive noise [19], [39], [40], or its burstiness, i.e., the side information on the impulsive noise arrival time [30], [41]. However, we will show in Section VIII that such lower bound can be approached by more practical estimators, especially at very low signal-to-interference power ratio (SIR), which are obviously the cases of higher interest for high power ImpN removal.

B. Optimal Bayesian Estimator (OBE)

Let's first consider the case where y represents separately either the real or the imaginary part, $y_{q,R}[n]$ and $y_{q,I}[n]$, respectively, of the complex-valued signal $y_q[n] = y_{q,R}[n] + jy_{q,I}[n]$. Assuming a K -GMM of the noise, independence from the signal and lack of NSI, by exploiting only the knowledge of the signal and noise *pdfs*, the classical MMSE-optimal Bayesian estimator is expressed by [8]

$$\begin{aligned} \hat{x}_{\text{OBE}}(y) &= E_{X|Y}\{x\} = \frac{E_{X,Y|X}\{x\}}{f_Y(y)} \\ &= \frac{\sum_{k=0}^{K-1} p_k E_{X,Y_k|X}\{x\}}{f_Y(y)} = \frac{\sum_{k=0}^{K-1} \rho_k p_k G(y; \sigma_{y_k}^2)}{\sum_{k=0}^{K-1} p_k G(y; \sigma_{y_k}^2)} y, \quad (11) \end{aligned}$$

where the statistical independence between X and W has been exploited, $f_{Y|X}(y) = f_W(y-x)$, $G(y; \sigma_k^2) * G(y; \sigma_x^2) = G(y; \sigma_{y_k}^2)$, $*$ stands for the convolution operator, and $\sigma_{y_k}^2 = \sigma_x^2 + \sigma_k^2$ is the received power when the noise is generated according to its k th Gaussian component.

Eq. (11) highlights how the nonlinear OBE depends on the signal variance σ_x^2 and the variance of each noise component σ_k^2 , together with the associated occurrence probability p_k . Thus, comparing (11) with (9), the OBE may be interpreted as a nonlinear attenuator of the input, e.g., $\hat{x}_{\text{OBE}}(y) = \beta_{\text{OBE}}(y) y$, with an attenuation factor $\beta_{\text{OBE}}(y)$, defined as

$$\beta_{\text{OBE}}(y) = \frac{\sum_{k=0}^{K-1} \rho_k p_k G(y; \sigma_{y_k}^2)}{\sum_{k=0}^{K-1} p_k G(y; \sigma_{y_k}^2)} \quad (12)$$

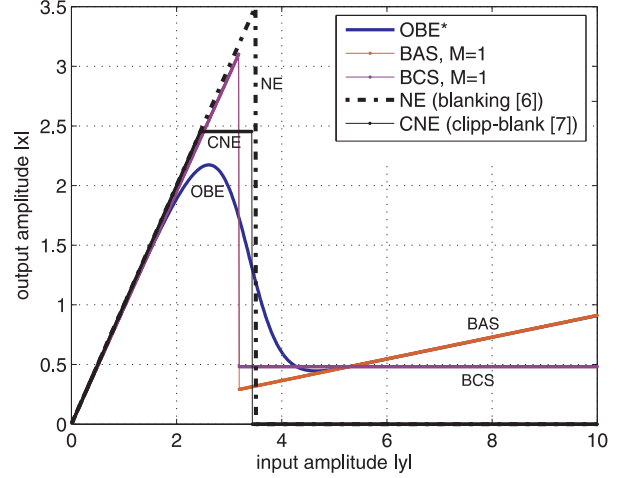


Fig. 2. Non-linear transfer functions of the optimal Bayesian estimator (OBE*) and the transfer functions of the proposed one-threshold ($M = 1$) based estimators BAS and BCS for the case of the two-component impulsive noise for $\text{SNR} = 25$ dB, $\text{SIR} = -10$ dB and $p_1 = 0.1$.

or, equivalently, as the weighted sum of the K linear attenuators $\rho_k y$ of the GAE in (9) by the non linear weights $p_k G(y; \sigma_{y_k}^2) / \sum_{k=0}^{K-1} p_k G(y; \sigma_{y_k}^2)$.

Expression (11) can be generalized to complex-valued signal $y = y_r + jy_i$ with straightforward similar derivations, ending up in²

$$x_{\text{OBE}^*}(y) = \frac{\sum_{k=0}^{K-1} \rho_k p_k G(|y|; \sigma_{y_k}^2)}{\sum_{k=0}^{K-1} p_k G(|y|; \sigma_{y_k}^2)} |y| e^{j \arg(y)}, \quad (13)$$

where the dependence on the *pdf* of the received signal amplitude $|y_k|$, conditional on the k th noise state, $f_{|Y_k|}(|y|)$ can be made explicit by substituting $G(|y|; \sigma_{y_k}^2) = f_{|Y_k|}(|y|) \sigma_{y_k}^2 / \sqrt{2\pi} |y|$ in (13). Assuming uncorrelated, independent, and asynchronous noise impulses, the *pdf* of the (conditional) received signal amplitude does not vary with time. On the other hand, when impulsive noise is correlated, bursty, synchronous or periodic, the $f_{|Y_k|}(|y|)$ *pdf*, and thus (13), varies from sample-to-sample. It is important to note that the assumption on uncorrelation and independence of the impulsive noise used in this work does not affect the correctness and efficiency of the presented methods.³ However, although this is not the subject of this manuscript, which focuses on low complexity techniques, we remark that it can be used to mitigate noise impulses more efficiently [41], [42].

IV. THRESHOLD-BASED BAYESIAN SUPPRESSORS

The shape of the OBE* in (13), shown for instance in Figs. 2–4, may be too complicated to be implemented by analog circuitry [8], [15] and, consequently, would call for a digital implementation after A/D conversion. However, implementation after A/D conversion would request a high number of bits

²we use OBE* in the following to denote OBE for the complex-valued signals.

³Note that communication systems affected by bursty noise regularly use interleaving techniques.

to conciliate the wide dynamic with a negligible quantization error. This fact, together with issues on computational complexity, system latency, and hardware cost, may suggest to look for alternative simpler estimators, to be implemented before A/D conversion. This is particularly true for time-varying fading channels where the useful signal variance σ_x^2 and the noise parameters $\{p_k, \sigma_k^2\}_{k=0, \dots, K-1}$ may change quite frequently and, consequently, the instantaneous NIS would request adaptive optimization of its shape. Therefore, in the following sections we propose and analyze suboptimal NISs based on multiple thresholding. Among these NISs, we will also consider a threshold-based clipping suppressor that is reminiscent of the estimator proposed in [15]. However, it should be emphasized that [15] shows practical results only for step-wise constant basis expansion model (BEM) (i.e., quantizers) with non-Gaussian noise that, differently from this manuscript, is not modeled as a Gaussian mixture. Furthermore, [15] proposes either to work with equi-spaced thresholds within the signal dynamic, or to optimize them according to quantization arguments with the Lloyd-Max algorithm. However this manuscript, not only considers a more general class of BEM functions to counteract a K-GMM noise, but it also proposes some alternative heuristic criteria to set the thresholds, as described in Sect. VI. Interestingly, this approach allows a closed form computation of the thresholds, which result to be slightly suboptimal with respect to the MMSE-optimal thresholds.

In the light of the BEM in [15], the suboptimal threshold-based estimators can be expressed as the linear combination of $M + 1$ known functions

$$\hat{x}(y) = \sum_{m=0}^M \beta_m v_m(|y|) e^{j \arg(y)}, \quad (14)$$

where β_m are $M + 1$ opportune scaling coefficients, $v_m(\cdot)$ are orthogonal functions, each one with non-overlapping support on the m th interval $I_m = [A_m, A_{m+1}[$, and among the $M + 2$ thresholds, only M are to be designed, because $A_0 = 0$, and $A_M = +\infty$ are actually signal envelope boundaries. In realistic applications, the optimal number of thresholds M can be determined as a trade-off between the system performance and the suppressor complexity. Higher M means more complicated analog circuitry of the suppressor, however, as shown in Sect. VIII, increasing M leads to a higher system performance.

A. Bayesian Attenuating Suppressor (BAS)

The attenuating suppressor performs a linear attenuation in each of the $M + 1$ regions as expressed by

$$\hat{x}_{\text{BAS}}(y) = \beta_m |y| e^{j \arg(y)}, \quad |y| \in [A_m, A_{m+1}[, \quad (15)$$

for $m = 0, \dots, M$. Note that a BAS with a single free-threshold (i.e., $M = 1$) shown in Fig. 2, with $\beta_0 = 1$ and $\beta_1 = 0$, corresponds to the impulse noise blanker (denoted as NE) analyzed in [6].

Following the general expression (14), the proposed M -threshold BAS is defined by

$$v_m^{(\text{BAS})}(y) = y u_m(y), \quad m = 0, \dots, M \quad (16)$$

where $u_m(y)$ is the unit box function

$$u_m(y) = \begin{cases} 1, & \text{if } y \in I_m \\ 0, & \text{otherwise} \end{cases}, \quad (17)$$

and I_m is the support of the m th function. Thus, the $M + 1$ -level BAS is given by

$$\hat{x}_{\text{BAS}}(y) = \sum_{m=0}^M \beta_m y u_m(|y|), \quad (18)$$

where the coefficients β_m are the attenuation factors. The closed-form expression for the optimal β_m is derived in Sect. VII.

B. Bayesian Clipping Suppressor (BCS)

The BCS is defined as

$$\hat{x}_{\text{BCS}}(y) = \begin{cases} \beta_0 y, & |y| < A_0 \\ \hat{x}_m e^{j \arg(y)}, & |y| \in [A_m, A_{m+1}[, \end{cases} \quad (19)$$

for $m = 1, \dots, M$. Note that, when $M = 2$ the suboptimal three-level estimator, with $\beta_0 = 1$, $\hat{x}_1 = A_1$, and $\hat{x}_2 = 0$, corresponds to the clipping-blanking method (in Fig. 2 denoted as CNE) proposed in [7].

Based on the general expression (14), the m th orthogonal function of the BCS is expressed by

$$v_m^{(\text{BCS})}(y) = \begin{cases} y u_0(y), & \text{if } m = 0 \\ u_m(y), & \text{otherwise} \end{cases}. \quad (20)$$

Consequently, the $M + 1$ -level BCS can also be expressed by

$$\hat{x}_{\text{BCS}}(y) = \beta_0 y u_0(|y|) + \sum_{m=1}^M \hat{x}_m u_m(|y|) e^{j \arg(y)}, \quad (21)$$

where β_0 is the attenuation factor in the interval $I_0 = [0, A_1[$ and \hat{x}_m is the clipping level in the m th interval. The closed-form expressions for the optimal β_0 and \hat{x}_m are derived in Sect. VII.

In the following sections we describe criteria to set the threshold values A_m , the attenuation factors β_m , and the clipping values \hat{x}_m of the BAS and the BCS, in order to maximize the output SNR, while preserving analytical closed form expressions. Some results are anticipated in Fig. 3 and Fig. 4, which, for specific values of the noise parameters, compare the shape of the proposed BAS and BCS, for $M = 1$ and $M = 5$, with the shape of the OBE*.

V. SIGNAL-TO-NOISE RATIO AT THE OUTPUT OF THE DETECTOR

The signal at the output of any non-linear estimator $\hat{x} = g(y)$, with $y = x + w$, can be expressed as [43]–[45]

$$\hat{x} = g(x + w) = \alpha_g x + d, \quad (22)$$

where $\alpha_g x$ represents the scaled version of the information-bearing signal at the input, and d is the distortion term that is uncorrelated with x , i.e., $E\{d x^*\} = 0$. Thanks to uncorrelation, the output SNR for any NIS $\hat{x} = g(y)$ is defined as

$$\text{SNR}_{\text{out}}^{(g)} = \frac{E\{|\alpha_g x|^2\}}{E\{|\hat{x} - \alpha_g x|^2\}} = \frac{\alpha_g^2}{E\{|\hat{x}|^2\}/2\sigma_x^2 - \alpha_g^2} \quad (23)$$

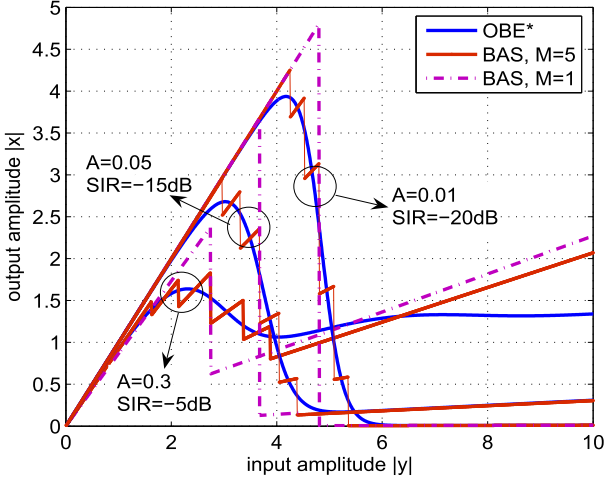


Fig. 3. Non-linear transfer functions of the optimal Bayesian estimator (OBE*), and the suboptimal transfer functions of the proposed M-threshold attenuating estimators (BAS) for Class-A ImpN model.

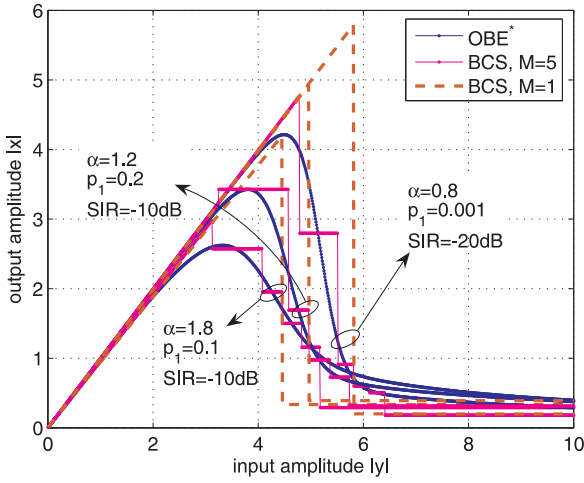


Fig. 4. Non-linear transfer functions of the optimal Bayesian estimator (OBE*), and the suboptimal transfer functions of the proposed M-threshold clipping estimators (BCS) for $S\alpha S$ ImpN model.

where $E\{|\hat{x}|^2\} = E\{|g(y)|^2\}$ represents the signal power at the output of the non-linear memoryless processor and $\alpha_g = E\{g(y)y^*\}/\sigma_y^2$ is the scaling factor imposed by the input-output cross-correlation[46]. In the following we derive the $\text{SNR}_{\text{out}}^{(g)}$ for the detectors mentioned so far, when the additive noise w is characterized by the K-GMM *pdf* in (4).

A. Genie-Aided Estimator

Since mixture components are mutually exclusive, the signal power at the GAE output and the attenuation coefficient α_g are simply expressed by $E\{|\hat{x}_{\text{GAE}}|^2\} = \sum_{k=0}^{K-1} p_k \beta_k^2 \sigma_{y_k}^2$ and $\alpha_{\text{GAE}} = \sum_{k=0}^{K-1} p_k \beta_k$, respectively. Thus, according to (23), the output SNR for the GAE is expressed by

$$\text{SNR}_{\text{out}}^{(\text{GAE})} = \frac{\left[\sum_{k=0}^{K-1} p_k \beta_k \right]^2}{\sum_{k=0}^{K-1} p_k (1 + \gamma_k) \beta_k^2 - \left[\sum_{k=0}^{K-1} p_k \beta_k \right]^2} \quad (24)$$

B. Bayesian Attenuating Suppressor

The BAS with M thresholds shown in Fig. 3, is characterized by an average output power⁴

$$E\{\hat{x}_{\text{BAS}}^2\} = \sum_{m=0}^M \beta_m^2 \sum_{k=0}^{K-1} p_k \int_{A_m}^{A_{m+1}} y^2 f_{Y_k}(y) dy, \quad (25)$$

By straightforward integration rules, involving a Rayleigh *pdf*, (25) leads to

$$\frac{E\{\hat{x}_{\text{BAS}}^2\}}{2\sigma_x^2} = \sum_{m=0}^M \beta_m^2 \sum_{k=0}^{K-1} p_k (1 + \gamma_k) (a_{m,k} - a_{m+1,k}), \quad (26)$$

where $a_{m,k} = (1 + A_m^2/\sigma_{y_k}^2) e^{-A_m^2/\sigma_{y_k}^2}$.

Similarly, the attenuation factor

$$\begin{aligned} \alpha_{\text{BAS}} &= \frac{E\{\hat{x}_t y_t^*\}}{\sigma_y^2} = \iint \hat{x}_t y_t^* f(\hat{x}_t, y_t^*) d\hat{x}_t dy_t^* \\ &= \sum_{m=0}^M \beta_m \sum_{k=0}^{K-1} p_k \int_{A_m}^{A_{m+1}} y^2 f_{Y_k}(y) dy \\ &= 2\sigma_x^2 \sum_{m=0}^M \beta_m \sum_{k=0}^{K-1} p_k (a_{m,k} - a_{m+1,k}). \end{aligned} \quad (27)$$

Thus, by direct substitution of (26) and (27) in (23), we obtain the BAS output SNR, expressed by,

$$\text{SNR}_{\text{out}}^{(\text{BAS})} = \frac{\alpha_{\text{BAS}}^2}{E\{\hat{x}_{\text{BAS}}^2\}/2\sigma_x^2 - \alpha_{\text{BAS}}^2}. \quad (28)$$

C. Bayesian Clipping Suppressor

The output signal power of the BCS in (19) is expressed by

$$\begin{aligned} E\{\hat{x}_{\text{BCS}}^2\} &= \int_0^{A_1} |\beta_0 y|^2 f_Y(y) dy + \sum_{m=1}^M \int_{A_m}^{A_{m+1}} \hat{x}_m^2 f_Y(y) dy \\ &= \beta_0^2 \sum_{k=0}^{K-1} p_k \int_0^{A_1} y^2 f_{Y_k}(y) dy \\ &\quad + \sum_{m=1}^M \hat{x}_m^2 \sum_{k=0}^{K-1} p_k \int_{A_m}^{A_{m+1}} f_{Y_k}(y) dy \end{aligned} \quad (29)$$

By straightforward integration, (29) leads to

$$\begin{aligned} \frac{E\{\hat{x}_{\text{BCS}}^2\}}{2\sigma_x^2} &= \beta_0^2 \sum_{k=0}^{K-1} p_k (1 + \gamma_k) (a_{k,0} - a_{k,1}) \\ &\quad + \sum_{m=1}^M \hat{x}_m^2 \sum_{k=0}^{K-1} p_k (1 + \gamma_k) P_{m,k} \end{aligned} \quad (30)$$

⁴for simplicity in the following we use \hat{x}_t, y_t for complex-valued signals and \hat{x}, y for their magnitudes $|\hat{x}_t|$ and $|y_t|$, respectively.

where $P_{m,k} = e^{-A_m^2/\sigma_{y_k}^2} - e^{-A_{m+1}^2/\sigma_{y_k}^2}$. Similarly,

$$\begin{aligned} \alpha_{\text{BCS}} &= \frac{E\{\hat{x}_t y_t^*\}}{\sigma_y^2} = \iint \hat{x}_t y_t^* f_{\hat{X}_t Y_t}(\hat{x}_t, y_t) d\hat{x}_t dy_t^* \\ &= \beta_0 \sum_{k=0}^{K-1} p_k \int_0^{A_1} f_{Y_k}(y) dy \\ &\quad + \sum_{m=1}^M \hat{x}_m \sum_{k=0}^{K-1} p_k \int_{A_m}^{A_{m+1}} y f_{Y_k}(y) dy. \end{aligned} \quad (31)$$

If we denote the average value of the observed output in the m th threshold interval when the k th noise mixture is active with $\bar{y}_{m,k}$, it can be expressed as

$$\begin{aligned} \bar{y}_{m,k} &= \int_{A_m}^{A_{m+1}} y f_{Y_k}(y) dy \\ &= A_m e^{-A_m^2/\sigma_{y_k}^2} - A_{m+1} e^{-A_{m+1}^2/\sigma_{y_k}^2} \\ &\quad - \sqrt{\pi} \sigma_{y_k} \left[\text{erf}\left(\frac{A_m}{\sigma_{y_k}}\right) - \text{erf}\left(\frac{A_{m+1}}{\sigma_{y_k}}\right) \right]. \end{aligned} \quad (32)$$

When we substitute (32) in (31), we obtain the following expression for the scaling factor

$$\alpha_{\text{BCS}} = \beta_0 \sum_{k=0}^{K-1} p_k (a_{0,k} - a_{1,k}) + \sum_{m=1}^M \hat{x}_m \sum_{k=0}^{K-1} p_k \bar{y}_{m,k}. \quad (33)$$

Thus, by direct substitution of (30) and (33) in (23), we obtain the output SNR for the BCS, expressed by

$$\text{SNR}_{\text{out}}^{(\text{BCS})} = \frac{\alpha_{\text{BCS}}^2}{E\{\hat{x}_{\text{BCS}}^2\}/2\sigma_x^2 - \alpha_{\text{BCS}}^2}. \quad (34)$$

Noteworthy, a closed-form analytical expression for the output SNR of the OBE* in (13) is not available [8], and consequently (28), or (34), could be used to approximate $\text{SNR}_{\text{out}}^{(\text{OBE}^*)}$ when the number M of thresholds is sufficiently high, and the associated threshold intervals are appropriately distributed over the dynamic range (e.g., $f_{|Y|}(y)$) of the observed signal y . Indeed, as proved in [15], any BEM-based estimator, whose threshold intervals $A_{m+1} - A_m$ vanish to zero when $M \rightarrow \infty$, converges to the OBE when $M \rightarrow \infty$. Further note that (24), (28), (34) are valid expressions for any set of thresholds values $\{A_m\}_{m=0,\dots,M}$, and any set of attenuating or clipping parameters $\{\beta_m\}_{m=0,\dots,M}$, $\{\hat{x}_m\}_{m=1,\dots,M}$, respectively, which influence the output SNRs by (27)–(26), or (33)–(30). In the next Sections we will address the problem of designing threshold and attenuating/clipping parameters in order to maximize the output SNR performance.

VI. OPTIMAL THRESHOLDING

Optimal thresholding-based NISs, would require joint optimization of the thresholds $\{A_m\}$, and of the attenuating/clipping factors $\{\beta_m\}$, $\{\hat{x}_m\}$, according to

$$\arg \max_{\{A_{m+1}, \beta_m, \hat{x}_m\}} \left\{ \text{SNR}_{\text{out}}^{(g)} \right\}, \quad m = 0, \dots, M. \quad (35)$$

However, even the optimization of a single-threshold of the BAS with fixed coefficients $\beta_0 = 1$ and $\beta_1 = 0$, which corresponds to the blanker in [6], is problematic. Indeed, the underlying optimization problem

$$A_1^* = \arg \max_{A_1} \left\{ \text{SNR}_{\text{out}}^{(\text{BAS})} \right\} \quad (36)$$

$$\text{s.t. } M = 1, A_0 = 0, A_2 = \infty, \beta_0 = 1, \beta_1 = 0,$$

does not admit a closed form analytical solution, and has to be computed numerically as in [6], or equivalently by iterative fixed-point algorithms, as in [8], [15].

Thus, in this manuscript we propose a suboptimal approach where first the thresholds $\{A_m\}$ are heuristically optimized, and successively each coefficient β_m and \hat{x}_m is optimized as detailed in Sect. VII. Specifically, we propose a novel, albeit meaningful criterion to set the thresholds, which has the nice property to allow their closed form computation and, at the same time, it is slightly suboptimal in output SNR with respect to the BAS, or the BCS, designed according to (35). To this end let's start considering the simplest BAS, i.e., the estimator with $M = 1$, $A_0 = 0$, $A_1 \in]0, \infty[$, and $A_2 = \infty$.

A. Single Threshold Selection for a Two-Component Impulsive Noise

For the simplest 2-GMM noise, the 2-level BAS has to choose the threshold A_1 according to some criterion. It can be compared to the GAE in (10), which switches among two linear attenuation coefficients $\{\beta_i\}_{i=0,1}$ according to the (perfect) knowledge of the noise state σ_w^2 , or σ_I^2 for a 2-GMM noise. The 2-level BAS can be interpreted as a sub-optimal estimator that chooses the estimation coefficient β_0 when the received amplitude $|y|$ is below a given threshold A_1 , and β_1 alternatively. This corresponds to use of the amplitude $|y|$ to decide whether the noise is in state $H_0 = \{w : \sigma_w^2 = \sigma_0^2\}$ or in $H_1 = \{w : \sigma_w^2 = \sigma_I^2\}$, and the overall problem can be casted as a binary hypothesis testing (HT), expressed by

$$\hat{x}_{\text{BAS}}(y) = \begin{cases} \beta_0 y, & \hat{H} = H_0 \\ \beta_1 y, & \hat{H} = H_1 \end{cases} = \begin{cases} \beta_0 y, & |y| \leq A_1 \\ \beta_1 y, & |y| > A_1. \end{cases} \quad (37)$$

As well known, such a binary HT is subject to two kinds of errors, with associated probabilities $P_{10} = P\{\hat{H} = H_1 | H_0\}$, $P_{01} = P\{\hat{H} = H_0 | H_1\}$, and the most powerful test in a Neyman-Pearson sense [47], [48] is the likelihood ratio test (LRT)

$$L(y) = \frac{f(y|H_1)}{f(y|H_0)} \underset{H_0}{\overset{H_1}{\gtrless}} \lambda_t \quad (38)$$

which decides to be in $\{H_1\}$ or $\{H_0\}$ when the LRT is greater or lower than a threshold λ_t . Fixing λ_t corresponds to fixing A_1 and viceversa. The two error probabilities P_{01} and P_{10} vary, in an opposite way, for different values of the threshold λ_t (A_1): the plot of the pairs $(1 - P_{01}, P_{10})$ on a cartesian plane for $\lambda_t \in [0, \infty]$ gives rise to the so called receiver operating characteristic (ROC) curve [48]. A Bayesian formulation of the test corresponds to associating a cost (return) to any possible

decision (correct and erroneous) and finding the threshold A_1 that minimizes the average cost (or inverse return).

It turns out that the optimization of any average return/cost function, such as the maximum SNR in (35) or the MSE, boils down to the LRT problem in (38) with a specific value of the threshold λ_t , which depends on the specific cost function and on the error probabilities P_{10} and P_{01} [48]. Thus, the maximum-SNR criterion to set the threshold, corresponds to a specific point on the ROC curve, which unfortunately does not admit a closed form solution for the computation of A_1 . An alternative working point on the ROC, but still a meaningful Bayesian approach, is to associate an equal cost to the two detection errors $\{\hat{H} = H_1|H_0\}$ and $\{\hat{H} = H_0|H_1\}$, and a zero-cost to the correct decisions $\{\hat{H} = H_1|H_1\}$ and $\{\hat{H} = H_0|H_0\}$. In this case, it is well known that the optimal threshold in (38) is $\lambda_t = p_0/p_1$ [48], i.e., the ratio among the (known) a priori probabilities for the noise to be either in thermal state H_0 , or in the impulsive state H_1 . Note that, in this case (38) clearly represents the maximum a-posteriori (MAP) noise detector, or the maximum-likelihood noise detector when $p_0 = p_1$. Thus, finding the threshold A_1 according to the boundary condition in (38) corresponds to

$$A_1 = \arg \left\{ p_0 f_{|Y_0|}(y) = p_1 f_{|Y_1|}(y) \right\}. \quad (39)$$

Interestingly, substituting in (39) the Rayleigh *pdfs* $f_{|Y_i|}(y)$ with variances $\sigma_{y_i}^2 = 2(1 + \gamma_i)\sigma_x^2$ that characterize the received signal under hypothesis H_0 and H_1 , it is possible to compute A_1 in closed-form, as expressed by

$$A_1 = \sqrt{2}\sigma_x \sqrt{\frac{(1 + \gamma_0)(1 + \gamma_1)}{\gamma_1 - \gamma_0} \log \left[\frac{p_0(1 + \gamma_1)}{p_1(1 + \gamma_0)} \right]}. \quad (40)$$

As we will show in Sect. VIII, the threshold A_1 in (40) is slightly suboptimal in output SNR with respect to the maximum-SNR strategy, for a wide range of interest of the impulsive noise parameters $\{A, \Gamma, \sigma_w^2\}$.

B. Single Threshold Selection for K -Component Impulsive Noise

In the case of the K-GMM we would like to detect the presence of one of the $K - 1$ impulsive noise components with respect to the thermal component with $k = 0$. Assuming that $\{\gamma_k\}_{k=0,1,\dots,K-1}$ increases with index k for the K-GMM impulsive noise, the use of the LRT criterion in (38) with $\lambda_t = p_0/p_k$, would suggest for each of the $K - 1$ impulsive components a different threshold A_k that, similarly to (39), would be expressed by

$$A_k = \sqrt{2}\sigma_x \sqrt{\frac{(1 + \gamma_0)(1 + \gamma_k)}{\gamma_k - \gamma_0} \log \left[\frac{p_0(1 + \gamma_k)}{p_k(1 + \gamma_0)} \right]}. \quad (41)$$

Anyway, in order to work with a 2-level detector, taking into account that the system will experience each of the mutually exclusive $K - 1$ impulsive contributions with a certain probability p_k , in order to choose the single free threshold, a heuristic albeit (due to exclusivity) quite reasonable criterion is to choose a probabilistic average of all the thresholds in (41), as

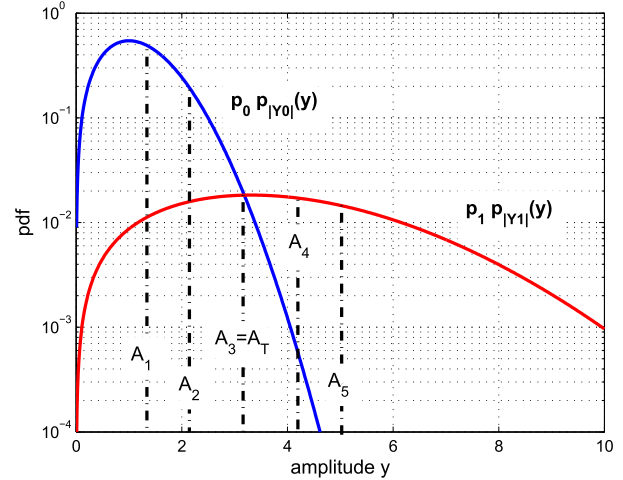


Fig. 5. $M = 5$ -thresholding for two-component impulsive noise (example for SIR = -10 dB, $p_1 = 0.1$ and SNR = 25 dB)

expressed by

$$A_T = \frac{1}{1 - p_0} \sum_{k=1}^{K-1} p_k A_k \quad (42)$$

C. M -Thresholding for Two-Component Impulsive Noise

For a given signal statistics, a possible set of M free thresholds $\{A_m\}_{m=1,\dots,M}$ could be computed by applying the Lloyd-Max optimal quantization algorithm [49] to the signal *pdf*. However, the Lloyd-Max solution does not admit a closed-form for any arbitrary distribution. Additionally, as highlighted in [15], the solution only exploits the statistical knowledge of the useful signal, ignoring the noise statistics. Thus, in the following we propose a heuristic approach to extend the formulation of the single-threshold optimization problem in (40) that, on top of its theoretical foundation, has the merit to allow a closed-form solution. First, we fix the middle-threshold A_T identical to the single threshold identified by (40). Specifically, for M odd it holds $A_T = A_{\lceil M/2 \rceil}$ and for M even the middle-threshold A_T is a fictitious threshold which is actually not used. Then, we generalize the criterion in (39) by defining a different scaled density ratio r_m for each threshold A_m , as expressed by

$$r_m = \frac{p_1 f_{|Y_1|}(A_m)}{p_0 f_{|Y_0|}(A_m)}, \quad (43)$$

which represents, for increasing m , an increasing confidence to be in H_1 , rather than in H_0 . To clarify the rationale behind the proposed approach, Fig. 5 illustrates the scaled densities $p_0 p_{|Y_0|}(y)$ and $p_1 p_{|Y_1|}(y)$ for the case $p_0 = 0.9$, $p_1 = 0.1$, SIR = -10 dB, and SNR = 25 dB with depicted $M = 5$ free thresholds. The middle threshold A_3 is given by (40), where it holds $p_1 p_{|Y_1|}(y) = p_0 p_{|Y_0|}(y)$.

Thus according to (43), for any given confidence ratio r_m , the corresponding threshold A_m can be computed as

$$A_m = \sqrt{2}\sigma_x \sqrt{\frac{(1 + \gamma_0)(1 + \gamma_1)}{\gamma_1 - \gamma_0} \log \left[r_m \frac{p_0(1 + \gamma_1)}{p_1(1 + \gamma_0)} \right]}. \quad (44)$$

As already anticipated, (44) is a generalization of (40), and it is equivalent for $r_m = 1$. Obviously, by the proposed approach, the SNR optimization problem with respect to A_m can be casted in an equivalent optimization problem with respect to r_m , as expressed by

$$\arg \max_{\{r_1, r_2, \dots, r_M\}} \{\text{SNR}_{\text{out}}\}. \quad (45)$$

Unfortunately, closed-form expressions for the optimal ratios $\{r_m\}$ maximizing the output SNR, according to (45), do not exist. Thus, we resorted to a Monte Carlo (MC) approach where, in order to numerically identify the optimal ratios r_m , we simulated the effect on the OFDM Gaussian signal of interest, of both the channel and the 2-GMM impulsive noise in (4), by employing the BAS estimator defined in (18). The MC simulations included also drawing a large number of uniform random variables $\{r_m\}_{m=1,2,\dots,M}$ and calculating for each toss the free-thresholds $\{A_m\}_{m=1,2,\dots,M}$ from (44), the associated optimal attenuating factors $\{\beta_m\}_{m=0,1,\dots,M}$ from (51), and the corresponding output SNR from (28). Assuming an even number of M free thresholds ($A_0 = 0$, $A_{M+1} = \infty$), by searching for the event that gives the maximal output SNR, and assigning the corresponding ratios $\{r_m\}_{m=1,2,\dots,M}$, we figured out that optimal r_m -s, as relative measures, do not depend on the signal parameters including the probabilities p_0, p_1 and noise-to-signal ratios γ_0, γ_1 . Furthermore, the results of an MC analysis show that the ratio for the top threshold A_M can be closely approximated by the simple formula $r_M = 2^{M-1}$ and that it also holds true $r_m/r_{m-1} = 2^2$. Based on that, the near-optimal ratios r_m for the upper subset of $\lceil M/2 \rceil$ free-thresholds can be expressed by

$$r_m = 2^{(2m-M-1)}, \quad m = \left\lfloor \frac{M}{2} \right\rfloor + 1, \dots, M. \quad (46)$$

The MC simulation has also shown that, for $M \leq 5$, the lower subset of $\lfloor M/2 \rfloor$ thresholds are located almost symmetrically around the middle threshold A_T given by (42). This is intuitively understandable since the point $y = A_T$ is the inflexion point of the OBE function (13). Therefore, given (44), the lower subset of $\lfloor M/2 \rfloor$ thresholds can be safely approximated by

$$A_m = 2A_T - A_{M-m}, \quad m = 1, \dots, \left\lfloor \frac{M}{2} \right\rfloor. \quad (47)$$

As demonstrated in Sect. VIII B, the output SNR achievable by the BAS or BCS suppressors with $M = 5$ free-thresholds is close to the maximal output SNR obtained by the OBE.⁵

D. M -Thresholding of K -Component Gaussian Mixture

M free thresholds $\{A_{m,k}\}_{m=1,\dots,M,k=1,\dots,K-1}$ can be defined, for each mixture component index k , by equations (44), (45), and (47), exactly as for the 2-GMM case.

Then, in order to define a unique set of M $\{A_m\}_{m=1,\dots,M}$ thresholds for a K -GMM impulsive noise with mutually

⁵for $M > 5$ the lower thresholds A_m have to be computed by using the empiric formula $\hat{A}_m = (A_m - A_T)e^{-0.014M} + A_T$; $m = 1, \dots, \lfloor \frac{M}{2} \rfloor$, which is obtained by MSE fitting of the MC results.

exclusive components, we propose to use the mean of $\{A_{m,k}\}$, as expressed by

$$A_m = \frac{1}{1-p_0} \sum_{k=1}^{K-1} p_k A_{m,k}, \quad m = 1, \dots, M, \quad (48)$$

Note that the thresholds for the BCS scheme are equal to the thresholds for the BAS scheme. Actually, when $M > 1$, the first free-threshold of the BCS is fixed to $A_1 = A_T/1.4$ [7]. For $M = 1$ the single free-threshold for both the schemes is given by (42).

E. Adaptive Thresholding

As anticipated by (8), in frequency-selective fading channels CSI has to be exploited block-by-block. Indeed, in this case the received signal power is expressed by $\sigma_{y_q}^2 = G_q \sigma_x^2 + \sigma_w^2$, where $G_q = \sum_{l=0}^{L-1} |h_q[l]|^2$ is the power attenuation induced by the channel during the q -th OFDM block. Thus, assuming that G_q varies in a block-fading fashion, while the noise variance σ_w^2 is fixed, the threshold A_m should adapt their values by (41) and (42) according to the variation of

$$\gamma_k = \frac{\sigma_k^2}{G_q \sigma_x^2} \quad (49)$$

and, consequently, adapt the associated attenuating and clipping parameters by (51) and (55), as detailed in the following.

VII. OPTIMAL ATTENUATING FACTORS AND CLIPPING LEVELS

It has been proved (see eq. (41) in [15]) that, for any BEM-based estimator represented by (14), and any set of given free thresholds $\{A_m\}_{m=1,\dots,M}$, the MMSE- and MSNR-optimal coefficients β_m are expressed by

$$\beta_m = \frac{E_{XY} \{x v_m(|y|)\}}{E_Y \{v_m^2(|y|)\}} = \frac{E_{XY} \{x v_m(|y|)\}}{P_{v_m}}. \quad (50)$$

Actually, by conditional expectation and (11), (50) can be reformulated as

$$\beta_m = \frac{E_Y \{v_m(|y|) E_{X|Y} \{x\}\}}{P_{v_m}} = E_Y \left\{ g_{\text{OBE}}(y) \frac{v_m(|y|)}{P_{v_m}} \right\}, \quad (51)$$

which is nothing but an appropriate statistical average of the optimal OBE $g_{\text{OBE}}(y)$, within the m th interval $I_m = [A_m, A_{m+1}]$.

A. Optimal Attenuating Factors

According to (51) and (16), the optimal attenuating factors for the BAS in (18) are expressed by

$$\beta_m = \frac{\sum_{k=0}^{K-1} \rho_k p_k \int_{A_m}^{A_{m+1}} y^2 f_{Y_k}(y) dy}{\sum_{k=0}^{K-1} p_k \int_{A_m}^{A_{m+1}} y^2 f_{Y_k}(y) dy} = \frac{\sum_{k=0}^{K-1} \rho_k p_k P_{m,k}}{\sum_{k=0}^{K-1} p_k P_{m,k}}, \quad (52)$$

where

$$P_{m,k} = (a_{m,k} - a_{m+1,k}) \sigma_{y_k}^2 \quad (53)$$

is the average output power in the m th threshold interval, conditioned on the noise belonging to the k -th distribution, and $a_{m,k}$ is defined in (26).

B. Optimal Clipping Levels

According to (51) and (20), the optimal clipping factors for the BCS in (21) are expressed by

$$\hat{x}_m = \frac{\int_{A_m}^{A_{m+1}} g_{\text{OBE}}(y) f_Y(y) dy}{\int_{A_m}^{A_{m+1}} f_Y(y) dy} = \int_{-\infty}^{+\infty} g_{\text{OBE}}(y) f_{Y|I_m}(y) dy, \quad (54)$$

where $f_{Y|I_m}(y)$ is the *pdf* of y , conditional on the event $\{y : y \in I_m\}$. This fact suggests also a quite intuitive interpretation for the optimal clipping (i.e., quantized) estimator, which approximates the OBE with its expected value within each clipping interval. By substituting (11) in (54), the optimal clipping values \hat{x}_m can be computed in closed form by

$$\hat{x}_m = \frac{\sum_{k=0}^{K-1} \rho_k p_k \int_{A_m}^{A_{m+1}} y f_{Y_k}(y) dy}{F_Y(A_{m+1}) - F_Y(A_m)} = \sum_{k=0}^{K-1} \rho_k \frac{p_k}{P\{I_m\}} \bar{y}_{m,k}, \quad (55)$$

where $F_{Y_k}(y) = 1 - e^{-y^2/2\sigma_{y_k}^2}$, $F_Y(y) = \sum_{k=0}^{K-1} p_k F_{Y_k}(y)$ is the cumulative distribution function for the envelope of the received signal y , $P\{I_m\} = F_Y(A_{m+1}) - F_Y(A_m)$ is the probability to belong to the m -th clipping interval, and $\bar{y}_{m,k}$ is given by (32).

VIII. NUMERICAL AND SIMULATION RESULTS

This section compares numerical and simulation results obtained by the proposed NISs, when employed in an OFDM communication system, as summarized in Fig. 1. Specifically, we considered both Class-A and α -stable impulsive noises impairing a 4-QAM and 16-QAM OFDM in IEEE 802.11ah WiFi systems, which are widely deployed in large scale sensor networks, extended range hotspots, and outdoor Wi-Fi for cellular traffic offloading. The system has been analyzed both in case of the static non-selective channels (i.e., AWGN) and in the case of the frequency-selective (e.g., multipath) fading channels, with exponential power-delay profile. In this last case, adaptive and non-adaptive thresholding strategies have also been compared.

As demonstrated in [15] there is a clear equivalence of the maximum output SNR and MMSE estimation. Therefore, a lower bound for MSE is equivalent to the upper bound of SNR_{out} , which is considered in this paper and is shown to be guaranteed by the OBE.

A. Numerical Results

Fig. 6 shows the SNR_{out} loss of the M -threshold BAS with respect to the OBE, versus the number of thresholds. As expected, the maximal loss is at $M = 1$ and it amounts to about 0.5 dB at $\text{SIR} = -10$ dB. However, this loss is about ten times lower at $M = 5$ and amounts to about -0.05 dB. At $M = 100$ the SNR_{out} is very close to that obtained by the OBE. Note that the results presented in Fig. 6 are obtained for $p_1 = 0.1$. However, the loss for lower p_1 is noticeably lower. Dot-dash line shows that for $p_1 = 0.0001$ the one-threshold attenuation produces at most -0.04 dB loss at $\text{SIR} = -10$ dB. On the other side, for higher p_1 the SNR_{out} loss is only slightly higher (e.g. for $p_1 = 0.25$ is drawn with a dotted line).

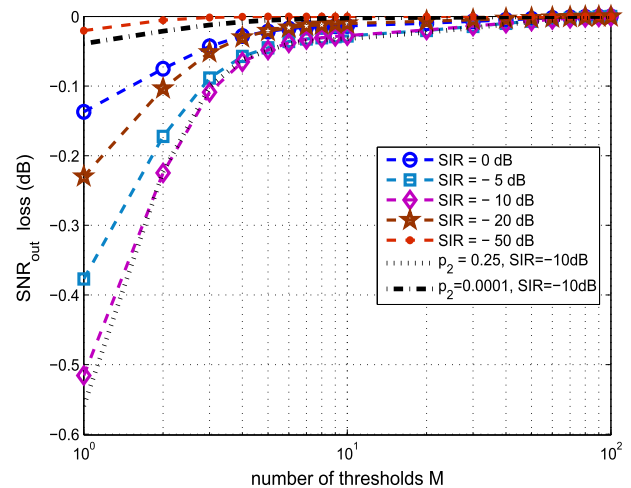


Fig. 6. SNR_{out} loss of the thresholding versus a number of thresholds M at $p_1 = 0.1$ and $\text{SNR} = 25$ dB.

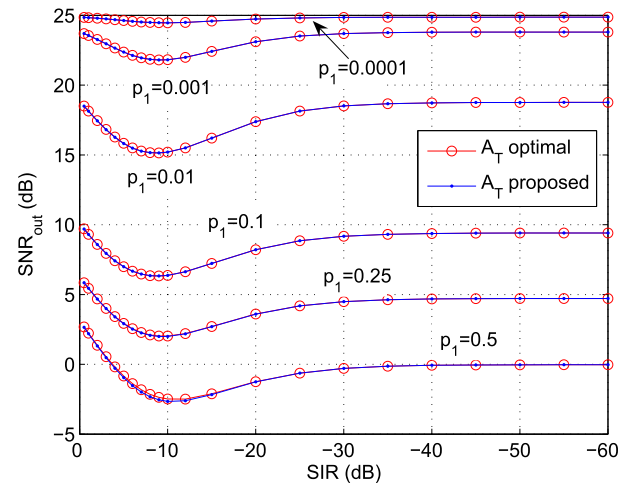


Fig. 7. SNR_{out} versus SIR for $\text{SNR} = 25$ dB and $p_1 = (0.0001, 0.001, 0.01, 0.1, 0.25, 0.5)$ for the optimal thresholds and the thresholds computed from (40).

Fig. 7 compares the BAS output SNR versus SIR, granted by the optimal and proposed sub-optimal thresholds for a 2-GMM with $\text{SNR} = 25$ dB and a set of impulsiveness probabilities $p_1 = \{0.0001, 0.001, 0.01, 0.1, 0.25\}$. The optimal thresholds that maximize the $\text{SNR}_{\text{out}}^{(\text{BAS})}$ are obtained by numerical solution of (35), while the sub-optimal thresholds are computed by (40). Evidently, the use of sub-optimal thresholds (40) does not reduce noticeably the system performance because the small shift from the optimal threshold is almost fully compensated by fitting the attenuation/clipping factors to the optimal ones, by (52) and (55). Therefore, the BAS thresholds we proposed by the closed-form expression (40) can be safely used to approximate the optimal ones.

Furthermore, Fig. 7 shows, that for the nulling estimator (NE) and clipping-nulling estimator (CNE), in the region $\text{SIR} > -15$ dB, the correct identification of the optimal thresholds is important, due to the relatively high sensitivity to small changes

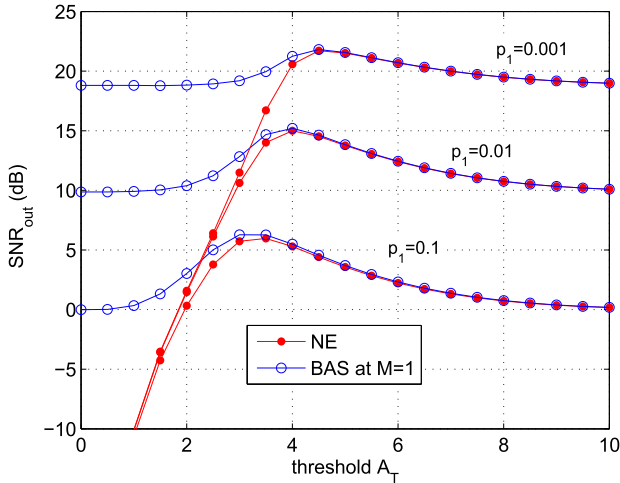


Fig. 8. SNR_{out} versus threshold A_T at optimal attenuation factor β_{opt} for $\text{SNR} = -10$ dB, at $p = 0.1, 0.01$ and 0.001 at $\text{SNR} = 40$ dB, and comparison of results for BAS and NE [6].

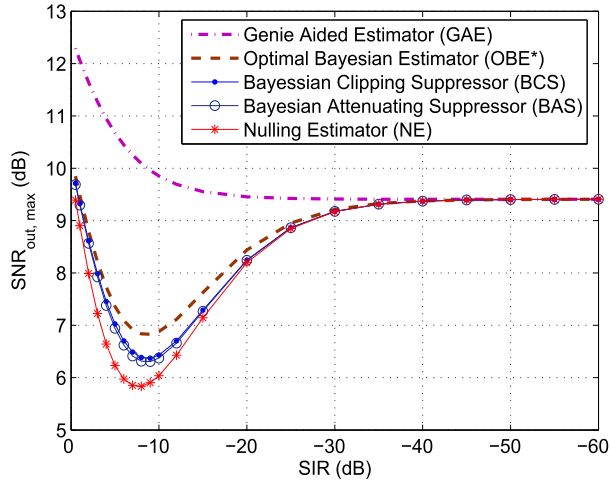


Fig. 9. Maximum achievable SNR_{out} at the output of the genie-aided estimator (GAE), optimal Bayesian estimator (OBE*), optimal one-threshold attenuator (BAS), optimal one-threshold clipper (BCS) and the optimal nulling estimator (NE) [6] versus SIR for $p_I = 0.1$ and $\text{SNR} = 25$ dB.

in the SIR. This effect is confirmed in Fig. 8, which compares the output SNR obtained by the BAS and the NE, for different threshold values; while the output SNR for the BAS is always greater than 0 dB for all the threshold values, this is not the case for the NE [6], which is characterized by an output SNR that steeply decreases for threshold values smaller than the optimal one (i.e. that optimizes the SNR_{out}).

Fig. 9 shows the BAS output SNR versus SIR for a 2-GMM impulsive noise, with impulsiveness probability $p_I = 1 - p_0 = 0.1$ and $\text{SNR} = 25$ dB. The figure compares the theoretical output SNR of the single free-threshold ($M = 1$) BAS and BCS, computed by (28) and (34), respectively, with the output SNR granted by the genie aided estimator (GAE) in (24), and by the OBE*. Due to the absence of a closed form expression, the output SNR for the OBE* is approximated by the output SNR

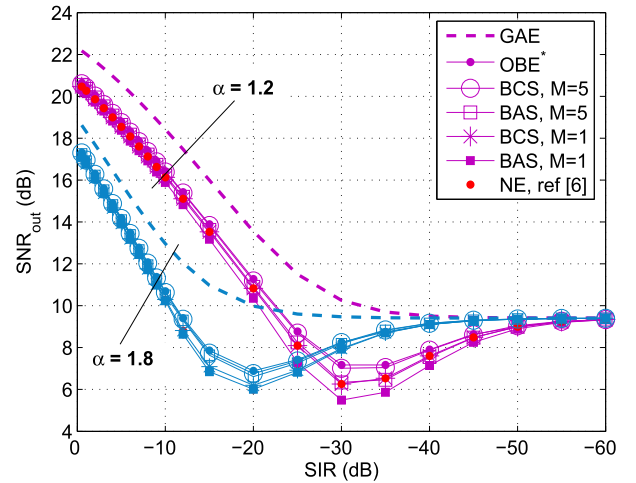


Fig. 10. Maximum achievable SNR_{out} at the output of the genie-aided detector (GAE), optimal Bayesian estimator (OBE*), optimal one-threshold attenuator (BAS), optimal one-threshold clipper (BCS) and the optimal nulling estimator (NE) [6] versus SIR for $S_{\alpha}S$ at $\alpha = 1.2, 1.8$ and $p_I = 0.1$ and $\text{SNR} = 25$ dB.

of the BAS in (28) for $M = 100$, e.g., due to the convergence of any BEM estimator to the OBE when $M \gg 1$ [15].

Noteworthy, for -20 dB $< \text{SIR} \leq 0$ dB the BAS and the BCS (even at $M = 1$) achieve a higher SNR_{out} than the NE in [6], while an even slightly higher SNR_{out} is obviously obtained by the OBE*. Clearly, the ideal GAE outperforms also the OBE*, up to 3 dB.

Fig. 10 shows the output SNR as a function of the SIR for $S_{\alpha}S$ impulsive noise with $\alpha = 1.2$ and 1.8 , impulsiveness probability $p_I = 1 - p_0 = 0.1$, and input $\text{SNR} = 25$ dB. The figure compares the output SNR obtained for the proposed single- and five-threshold BAS and BCS, with the output SNR obtained for the ideal GAE, the OBE* and the optimal NE [6]. Observing Fig. 10 it is possible to conclude that for $S_{\alpha}S$ noise, contrary to the Class-A, the BAS with a single free threshold $M = 1$ is somewhat inferior to the NE. This is due to the fact that the OBE* shape in this case is more similar to an NE rather than to a BAS [8]. This is also confirmed by the fact that in this case the better solution is the BCS that even with $M = 1$ provides a slightly higher output SNR than the NE, and a noticeably higher when $M = 5$. Noteworthy, the computation of the optimal nulling threshold for the NE requests numerical integration capabilities [6]–[9], which may be cumbersome in real-time applications with fast changing parameters.

B. Simulation Results

This subsection shows few examples of impulsive noise removal by BASs and BCSs, employing one to five free-thresholds, and compares their performance with the GAE, the OBE*, the NE [6], and the CNE in [7].

Fig. 11 shows the output SNR performance versus SIR of the single, two and five free-threshold BAS and BCS for a Class-A impulsive noise with $A = 0.1$ and $\text{SNR} = 25$ dB. The SNR_{out} results are compared with the results obtained for the GAE, the OBE*, the NE, and the CNE. Simulation results confirm that

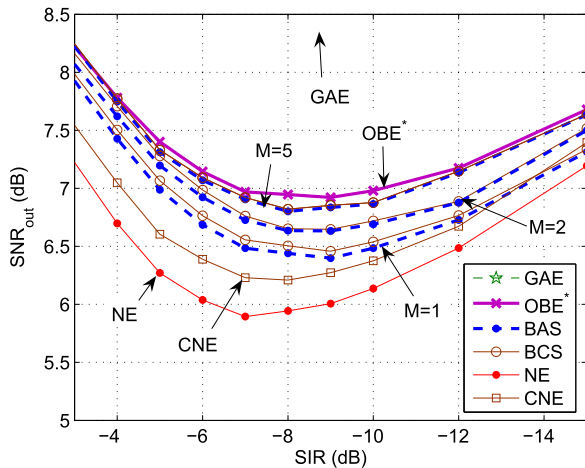


Fig. 11. SNR_{out} versus SIR for GAE, OBE*, CNE and NE compared with the optimal threshold-based methods BAS and BCS for $M = 1$, $M = 2$ and $M = 5$ (Class A ImpN with $A = 0.1$ and $\text{SNR} = 25$ dB).

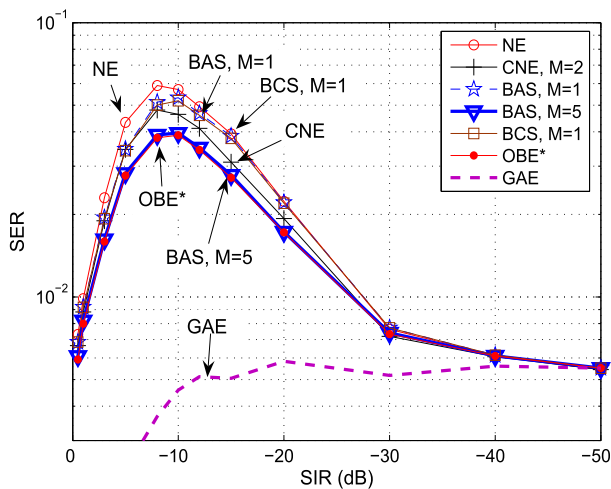


Fig. 12. SER performance versus SIR and its comparison with the one- and five-threshold attenuation (BAS) and clipping (BCS) with the ideal genie-aided estimator (GAE), the optimal Bayesian OBE*, the nulling (NE) and the clipping-nulling (CNE). OFDM 64-subcarrier, 16-QAM for $A = 0.01$ and $\text{SNR} = 25$ dB.

the highest output SNR is obtained by the GAE, which fully exploits the NSI. Without full NSI, the highest output SNR is obtained by the OBE*. Almost the same SNR_{out} as for OBE* is obtained by the five-threshold BAS and the five-threshold BCS. It is also interesting to note that BAS and BCS, even with a single (i.e., $M = 1$) threshold, offer a somewhat higher output SNR with respect to the two-threshold CNE.

Fig. 12 shows the SER performance versus SIR for a 16-QAM OFDM system with $N = 64$ subcarriers as in WiFi 802.11ah, affected by a Class-A impulsive noise, with $A = 0.01$ and input $\text{SNR} = 25$ dB. Simulation performance for single and five free-thresholds BAS and BCS are compared with those of the GAE, the OBE*, the NE, and the CNE. As expected, relative performance in terms of SER of the analyzed suppressors correspond to those in terms of output SNR, as shown in Fig. 11. Specifically, almost the same SER as for the OBE* is obtained by the five-threshold BAS and the five-threshold BCS.

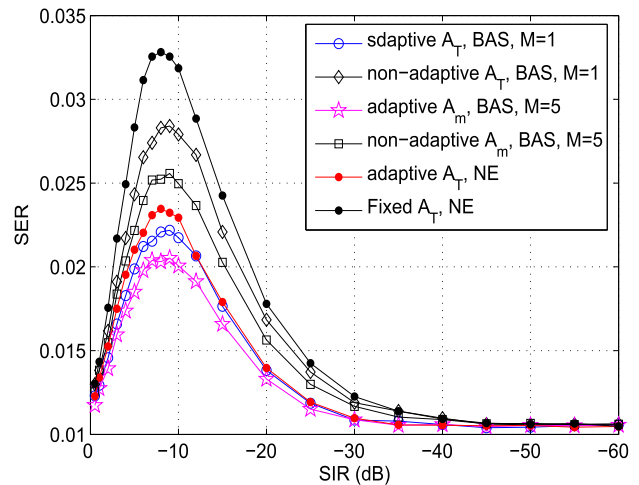


Fig. 13. Comparison of SER at the output of BAS for $M = 1$ and $M = 5$ for adaptive and non-adaptive schemes and comparison with the adaptive blanking scheme (adaptive-NE). 4-QAM OFDM for $A = 0.01$ and $\text{SNR} = 25$ dB.

Fig. 13 shows the SER performance for a 4-QAM OFDM system in a frequency selective Rayleigh fading channel with $L = 32$ paths, an exponential power-delay profile $\{\sigma_l^2 = 0.2835\exp(-l/3)\}_{l=0,\dots,L-1}$, and a Class-A impulsive noise. The figure shows the SER performance versus the SIR for $A = 0.01$ and $\text{SNR} = 25$ dB of the adaptive BAS with $M = 1$ and $M = 5$ thresholds, and compares them with those of the non-adaptive BAS suppressors. It can be further concluded that, for $\text{SIR} = -10$ dB, the adaptive schemes outperform regarding the non-adaptive ones, SER for about 20%. Similarly to the SER results shown in Fig. 12 for the AWGN channel and the non-adaptive schemes, the adaptive-BAS shows better performance for increasing number M of thresholds, and always outperforms the optimal NE defined in [6], [50]. This fact is more noticeable for SIR values above -20 dB and lower values of A . Furthermore, note that the adaptive-NE requires a numerical integration for each OFDM block, differently from the adaptive-BAS that only requires a simple closed-form recalculation, as discussed in Sect. VI-E. Finally, the SER results shown in Fig. 13 for $A = 0.01$ in the case of the frequency-selective fading channels, confirm the benefit of the adaptive strategies, with respect to the non-adaptive ones.

Note that the results presented in this section are obtained for a realistic scenario where the channel is affected by an uncorrelated impulsive noise or correlated and bursty noise. In this last case the system regularly uses interleaving/deinterleaving techniques. If the receiver does not use side information on the noise correlation, as assumed in this work, the best achievable performance is the one obtained by the OBE [15]. Thus, showing the performance comparison with respect to the conventional and the optimal OBE is particularly meaningful and testify the effectiveness of the proposed solutions.

IX. CONCLUSION

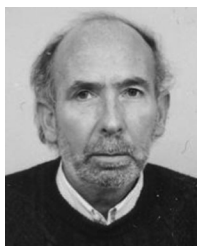
This paper has investigated optimal Bayesian estimation for OFDM signals, or Gaussian distributed information, in channels

interfered by Class-A and $S\alpha S$ impulsive noise. Since implementation of the optimal Bayesian estimator (OBE) by analog circuitry is rather complicated, we focused on multiple threshold-based estimators, including linear attenuators and clippers, which approximate the OBE. In order to enable flexible adaptation of the threshold-based estimators to time-varying channels, a special attention has been paid to develop closed-form expressions for all the estimator parameters, including the optimal thresholds, attenuating coefficients, and clipping levels. Simulation results have shown that the proposed attenuating and clipping estimators with only five thresholds achieve almost the same performance as the OBE. This result is not surprising because, as demonstrated in this paper, the piece-wise attenuating/clipping non-linear suppressor, with five almost optimal thresholds and attenuating/clipping factors, approximates the OBE non-linear function very well. It has also been shown that for Class-A impulsive noises, the single-threshold solutions outperform the well known optimal blanking (nulling) estimator in SER and output SNR, for the whole range of the impulsive noise parameters. Future work will focus on implementation of the proposed threshold-based suppressors on real analog circuitry, and on performance-complexity tradeoffs in practical application scenarios.

REFERENCES

- [1] D. Middleton, "Canonical and quasi-canonical probability models of class a interference," *IEEE Trans. Electromagn. Compat.*, vol. EMC-25, no. 2, pp. 76–106, May 1983.
- [2] D. Middleton, "Non-Gaussian noise models in signal processing for telecommunications: New methods and results for class a and class b noise models," *IEEE Trans. Inf. Theory*, vol. 45, no. 4, pp. 1129–1149, May 1999.
- [3] M. G. Sanchez, L. de Haro, M. C. Ramon, A. Mansilla, C. M. Ortega, and D. Oliver, "Impulsive noise measurements and characterization in a UHF digital TV channel," *IEEE Trans. Electromagn. Compat.*, vol. 41, no. 2, pp. 124–136, May 1999.
- [4] S. Zabin and H. Poor, "Efficient estimation of class a noise parameters via the em algorithm," *IEEE Trans. Inf. Theory*, vol. 37, no. 1, pp. 60–72, Jan. 1991.
- [5] H. A. Suraweera, C. Chai, J. Shentu, and J. Armstrong, "Analysis of impulse noise mitigation techniques for digital television systems," in *Proc. 8th Int. OFDM Workshop*, Lisbon, Portugal, Sep. 2003, pp. 172–176.
- [6] S. Zhidkov, "Performance analysis and optimization of OFDM receiver with blanking nonlinearity in impulsive noise environment," *IEEE Trans. Veh. Technol.*, vol. 55, no. 1, pp. 234–242, Jan. 2006.
- [7] S. Zhidkov, "Analysis and comparison of several simple impulsive noise mitigation schemes for OFDM receivers," *IEEE Trans. Commun.*, vol. 56, no. 1, pp. 5–9, Jan. 2008.
- [8] P. Banelli, "Bayesian estimation of a Gaussian source in middleton class-a impulsive noise," *IEEE Signal Process. Lett.*, vol. 20, no. 10, pp. 956–959, Oct. 2013.
- [9] P. Banelli and L. Rugini, "Impulsive noise mitigation for wireless OFDM," in *Proc. IEEE Int. Workshop Signal Process. Adv. Wireless Commun.*, Stockholm, Sweden, Jun./Jul. 2015, pp. 346–350.
- [10] D. Darsena, G. Gelli, F. Melito, and F. Verde, "ICI-free equalization in OFDM systems with blanking preprocessing at the receiver for impulsive noise mitigation," *IEEE Signal Process. Lett.*, vol. 22, no. 9, pp. 1321–1325, Sep. 2015.
- [11] P. Torio and M. G. Sanchez, "Elimination of impulsive noise by double detection in long-term evolution handsets," *IEEE Trans. Veh. Technol.*, vol. 64, no. 7, pp. 2875–2882, Jul. 2015.
- [12] E. E. Kuruoglu, C. Molina, and W. J. Fitzgerald, "Approximation of alpha-stable probability densities using finite Gaussian mixtures," in *Proc. 9th Eur. Signal Process. Conf.*, Rhodes, Greece, Sep. 1998, pp. 1–4.
- [13] H. N. Hamdan and J. P. Nolan, "Estimating the parameters of infinite scale mixtures of normals," in *Proc. 36th Symp. Interface, Comput. Sci. Statist.*, 2004, pp. 161–169.
- [14] N. Rozic, M. Russo, M. Saric, J. Radic, and D. Begusic, "Approximation of the symmetric alpha-stable density with mixture of scaled Gaussians, Univ. of Split, Split, Croatia, Tech. Rep. P023-02311924-060212, 2013. [Online]. Available: <http://lab405.fesb.hr/sas/>
- [15] L. Rugini and P. Banelli, "On the equivalence of maximum SNR and MMSE estimation: Applications to additive non-Gaussian channels and quantized observations," *IEEE Trans. Signal Process.*, vol. 64, no. 23, pp. 6190–6199, Dec. 2016.
- [16] K. S. Vastola, "Threshold detection in narrow-band non-Gaussian noise," *IEEE Trans. Commun.*, vol. 32, no. 2, pp. 134–139, Feb. 1984.
- [17] H. Oh and H. Nam, "Design and performance analysis on nonlinearity preprocessors in an impulsive noise environment," *IEEE Trans. Veh. Technol.*, vol. 66, no. 1, pp. 364–375, Jan. 2017.
- [18] P. Kyees, R. McConnell, and K. Sistanizadeh, "ADSL: A new twisted pair access to the information highway," *IEEE Commun. Mag.*, vol. 33, no. 4, pp. 52–60, Apr. 1995.
- [19] M. Nassar, J. Lin, and B. L. Evans, "Impulsive noise mitigation in power-line communications using sparse Bayesian learning," *IEEE J. Sel. Areas Commun.*, vol. 31, no. 7, pp. 1172–1183, Jul. 2013.
- [20] K. L. Blackard, T. S. Rappaport, and C. W. Bostian, "Measurement and models of radio frequency impulsive noise for indoor wireless communications," *IEEE J. Sel. Areas Commun.*, vol. 11, no. 7, pp. 991–1001, Sep. 1993.
- [21] E. G. Hamza, L. C. N. Azzaoui, F. Septier, and P. A. Rolland, " α -stable interference modeling and cauchy receiver for an IR-UWB ad hoc network," *IEEE Trans. Commun.*, vol. 58, no. 6, pp. 1748–1757, Jun. 2010.
- [22] Z. Wang and G. B. Giannakis, "Wireless multicarrier communications," *IEEE Signal Process. Mag.*, vol. 17, no. 3, pp. 29–48, May 2000.
- [23] P. Banelli and L. Rugini, "OFDM and multicarrier signal processing," in *Academic Press Library in Signal Processing: Communications and Radar Signal Processing*, vol. 2. Amsterdam, The Netherlands: Elsevier, 2014, pp. 187–293.
- [24] M. Ghosh, "Analysis of the effect of impulse noise on multicarrier and single carrier QAM systems," *IEEE Trans. Commun.*, vol. 44, no. 2, pp. 145–147, Feb. 1996.
- [25] H. Nikoodar and D. Nathoeni, "Performance evaluation of OFDM transmission over impulsive noisy channels," in *Proc. 13th Int. Symp. Pers. Indoor Mobile Radio Commun.*, Lisbon, Portugal, Feb. 2002, vol. 2, pp. 550–554.
- [26] S. A. Kassam, *Signal Detection in Non-Gaussian Noise*, New York, NY, USA: Springer-Verlag, 1988.
- [27] W. Feller, *An Introduction to Probability Theory and Its Application*, vol. II. New York, NY, USA: Wiley, 1971.
- [28] T. Nakai and Z. Kawasaki, "On impulsive noise from Shinkansen," *IEEE Trans. Electromagn. Compat.*, vol. EMC-25, no. 4, pp. 396–404, Nov. 1983.
- [29] A. P. Dempster, N. M. Laird, and D. B. Rubin, "Maximum likelihood from incomplete data via the EM algorithm," *J. Roy. Statist. Soc., Series B*, vol. 39, no. 1, pp. 1–38, 1977.
- [30] T. Y. Al-Naffouri, A. A. Quadeer, and G. Caire, "Impulse noise estimation and removal for OFDM systems," *IEEE Trans. Commun.*, vol. 62, no. 3, pp. 976–989, Mar. 2014.
- [31] S. Hur et al., "Proposal on millimeter-wave channel modeling for 5g cellular system," *IEEE J. Sel. Topics Signal Process.*, vol. 10, no. 3, pp. 454–469, Mar. 2016.
- [32] P. A. Delaney, "Signal detection in multivariate class a interference," *IEEE Trans. Commun.*, vol. 43, no. 2–4, pp. 365–373, Feb. 1995.
- [33] D. Middleton, "Statistical-physical models for electromagnetic interference," *IEEE Trans. Electromagn. Compat.*, vol. EMC-19, no. 3, pp. 106–127, Aug. 1977.
- [34] D. Middleton, "Procedures for determining the parameters of the first-order canonical models of class a and class b electromagnetic interference," *IEEE Trans. Electromagn. Compat.*, vol. EMC-21, no. 3, pp. 190–208, Aug. 1979.
- [35] M. Shao and C. Nikias, "Signal processing with fractional lower order moments: Stable processes and their applications," *Proc. IEEE*, vol. 81, no. 7, pp. 986–1010, Jul. 1993.
- [36] J. Gonzalez, J. Paredes, and G. Arce, "Zero-order statistics: A mathematical framework for the processing and characterization of very impulsive signals," *IEEE Trans. Signal Process.*, vol. 54, no. 10, pp. 3839–3851, Oct. 2006.

- [37] A. Achim and E. Kuruoglu, "Image denoising using bivariate α -stable distributions in the complex wavelet domain," *IEEE Signal Process. Lett.*, vol. 12, no. 1, pp. 17–20, Jan. 2005.
- [38] J. Proakis, *Digital Communications*, 5th ed. New York, NY, USA: McGraw-Hill, 2008.
- [39] D. Middleton, "Threshold detection in correlated non-Gaussian noise fields," *IEEE Trans. Inf. Theory*, vol. 41, no. 4, pp. 976–1000, Jul. 1995.
- [40] B. M. Sadler, "Detection in correlated impulsive noise using fourth-order cumulants," *IEEE Trans. Signal Process.*, vol. 44, no. 11, pp. 2793–2800, Nov. 1996.
- [41] D. Fertonani and G. Colavolpe, "On reliable communications over channels impaired by bursty impulse noise," *IEEE Trans. Commun.*, vol. 57, no. 7, pp. 2024–2030, Jul. 2009.
- [42] G. Ndo, F. Labeau, and M. Kassouf, "A Markov-middleton model for bursty impulsive noise: Modeling and receiver design," *IEEE Trans. Power Del.*, vol. 28, no. 4, pp. 2317–2325, Oct. 2013.
- [43] R. Price, "A useful theorem for nonlinear devices having Gaussian inputs," *IRE Trans. Inf. Theory*, vol. 4, no. 2, pp. 69–72, 1958.
- [44] J. J. Busgang, "Cross correlation function of amplitude-distorted Gaussian signals," Cambridge, MA, USA, MIT, Tech. Rep. 216, Mar. 1952.
- [45] J. Minkoff, "The role of AM-to-PM conversion in memoryless nonlinear systems," *IEEE Trans. Commun.*, vol. C-33, no. 2, pp. 139–144, Feb. 1985.
- [46] P. Banelli and S. Capobardi, "Theoretical analysis of performance of OFDM signals in non-linear AWGN channels," *IEEE Trans. Commun.*, vol. 48, no. 3, pp. 430–441, Mar. 2000.
- [47] A. Spalding and D. Middleton, "Optimum reception in an impulsive interference environment-Part I coherent detection," *IEEE Trans. Commun.*, vol. C-25, no. 9, pp. 910–923, Sep. 1977.
- [48] S. Kay, *Fundamentals of Statistical Signal Processing: Detection Theory*, vol. 2. Englewood Cliffs, NJ, USA: Prentice-Hall, 1993.
- [49] A. Gersho, "Quantization," *IEEE Commun. Mag.*, vol. 15, no. 5, pp. 16–29, Sep. 1977.
- [50] S. V. Zhidkov, "Impulsive noise suppression in OFDM-based communication systems," *IEEE Trans. Consum. Electron.*, vol. 49, no. 4, pp. 944–948, Nov. 2003.



Nikola Rožić (SM'13) received the B. S. degrees in electrical engineering and electronics from the University of Split, Split, Croatia, in 1968 and 1969, respectively, and the M.S. and Ph.D. degrees from the University of Ljubljana, Ljubljana, Slovenia, in 1977 and in 1980, respectively. Currently, he is a Professor emeritus in electrical and computer engineering and works with the research team for advanced networking technologies and systems at the FESB, University of Split. His research interest includes information and communication theory, signal processing, source and channel coding, and prediction methods and forecasting. Since 1998, he has been a TPC Co-Chair of the International Conference on Software, Telecommunications and Computer Networks (SoftCOM), which was technically cosponsored by IEEE Communications Society (ComSoc). He is the Editorial Chair of the *Journal of Communications Software and Systems*. He is a member of the IEEE Communications, Computer, Broadcasting, Antenna and Propagation, Information theory, and Signal Processing Societies. He is a Co-founder and the President of the Croatian Communications and Information Society (CCIS), which is the sister society of the IEEE ComSoc.



Paolo Banelli (S'90–M'99) received the Laurea degree (cum laude) in electronics engineering and the Ph.D. degree in telecommunications both from the University of Perugia, Perugia, Italy, in 1993 and 1998, respectively. In 2005, he was appointed as an Associate Professor with the Department of Electronic and Information Engineering, University of Perugia, where he has been an Assistant Professor since 1998. In 2001, he joined the SpinComm Group, ECE Department, University of Minnesota, Minneapolis, MN, USA, as a Visiting Researcher.

His research interests include statistical signal processing for wireless communications, with emphasis on multicarrier transmissions, signal processing for biomedical applications, spectrum sensing for cognitive radio, waveform design for 5G communications, and more recently graph signal processing. He was a member (2011–2013) of the IEEE Signal Processing Society's Signal Processing for Communications and Networking Technical Committee. In 2009, he was a General Co-Chair of the IEEE International Symposium on Signal Processing Advances for Wireless Communications. He served (2013–2016) as an Associate Editor for the IEEE TRANSACTIONS ON SIGNAL PROCESSING, and for the *EURASIP Journal on Advances in Signal Processing* since 2012.



Dinko Begušić (SM'13) received the B.S. degree in electrical engineering (concentration of telecommunications and informatics) from the University of Split, Split, Croatia, in 1983, and the M.S. and Ph.D. degrees in electrical engineering (telecommunications and informatics) from the University of Zagreb, Zagreb, Croatia, in 1988 and 1992, respectively. Since 1985, he has been with the Faculty of electrical engineering, mechanical engineering and naval architecture, University of Split, Croatia. He was a Visiting Researcher with the Université Libre

de Bruxelles and King's College London, and a Visiting Assistant Professor with the University of Texas at Dallas, Richardson, TX, USA. Since 2002, he has been appointed the Chair of communications technologies and signal processing. From 2004 to 2008, he was elected the Dean of the Faculty. His research interests include communication systems and networks, wireless and optical networks, digital signal processing and adaptive algorithms, and communications software. He is the leader of the research group for advanced networking technologies and systems. He is a Co-founder and Co-Editor-in-Chief of the *Journal on Communications Software and Systems*. He is a Co-founder and TPC Co-Chair of the international conference on Software, Telecommunications and Computer Networks SoftCOM.



Joško Radić (M'05) received the M.S. and Ph.D. degrees both in communications engineering from the University of Split, Split, Croatia, in 2005 and 2009, respectively. He is an Associate Professor with the Faculty of electrical engineering, mechanical engineering and naval architecture, University of Split, Split, Croatia. His academic work includes teaching at the undergraduate, graduate, and postgraduate study at the University of Split, in the field of communications. His scientific research interests include wireless communications, signal processing, multi-carrier systems, and coding theory. Currently, he is a Deputy Head of the Department for Electronics and Computing, Chair of Communications and Information Systems, General Financial Chair of the international conference on Software, Telecommunications and Computer Networks SoftCOM and an Area Editor for the *Journal of Communications Software and Systems*. He is a member of the IEEE Communications Society and the Croatian Communications and Information Society.